

The Crystal Structures of the Chevrel Phases $\text{Li}_{3.3}\text{Mo}_6\text{S}_8$ and $\text{Li}_{3.2}\text{Mo}_6\text{Se}_8$

R. J. CAVA, A. SANTORO,* AND J. M. TARASCON†

*Bell Laboratories, Murray Hill, New Jersey 07974 and *National Bureau of Standards, Washington, D.C. 20234*

Received November 7, 1983; in revised form February 1, 1984

The crystal structures of $\text{Li}_{3.3}\text{Mo}_6\text{S}_8$ and $\text{Li}_{3.2}\text{Mo}_6\text{Se}_8$, Chevrel phases formed by the insertion of lithium into Mo_6S_8 and Mo_6Se_8 , were determined by neutron diffraction powder profile analysis. The Mo_6S_8 and Mo_6Se_8 clusters are quite similar to those in other compounds of this type. The lithium atoms in both cases are disordered over the two concentric rings of available tetrahedrally coordinated small atom sites. For both compounds, occupancy of the outer ring is strongly preferred, and in $\text{Li}_{3.3}\text{Mo}_6\text{S}_8$ the inner lithium ring has a unique puckered geometry.

Introduction

The large class of ternary molybdenum chalcogenides of formula $M_y\text{Mo}_6X_8$ (M = metallic element, $0 \leq y \leq 4$, $X = \text{S, Se, Te}$) has been of great interest due to unusual superconducting properties and the extensive chemical variety of the "ternary element" M (1). The basic structural building blocks are Mo_6X_8 clusters consisting of eight X atoms forming the corners of a cube around an octahedron of six Mo atoms near the cube face centers. The ternary elements are located between the Mo_6X_8 clusters in positions which are near the line of the cluster cube diagonals (large m atoms), or displaced in sets of concentric rings centered about the cube diagonal (small ions). The small M ions may either be ordered or disordered in the rings.

The synthesis of single-phase materials of carefully controlled stoichiometry is unfortunately not generally a straightforward matter and thus discrepancies occur in the literature. Recently, new low-temperature synthesis techniques have been reported for a variety of these phases which largely overcomes difficulties in the synthesis of materials of known stoichiometry (2). The lithium-containing phases $\text{Li}_{3.3}\text{Mo}_6\text{S}_8$ and $\text{Li}_{3.2}\text{Mo}_6\text{Se}_8$ were synthesized by lithium insertion into Mo_6S_8 and Mo_6Se_8 by reaction with *n*-butyl lithium at ambient temperature and annealing for 5 days at 450°C to homogenize the lithium distribution. Chemical and X-ray diffraction analysis of the resulting products confirmed one of the sets of stoichiometries and crystallographic unit cell parameters previously reported (3, 10, 12, 13). (3.3Li/ Mo_6S_8 and 3.2Li/ Mo_6Se_8 by atomic absorption analysis (error $\pm 0.1/\text{F.U.}$)). In this study we have determined the crystal structures of $\text{Li}_{3.3}\text{Mo}_6\text{S}_8$ and

† Present affiliation: Bell Communications Research, Inc., Murray Hill, N.J.

$\text{Li}_{3,2}\text{Mo}_6\text{Se}_8$ by neutron diffraction powder profile analysis as used in the study of several lithium-inserted metal oxides (e.g., (4)). We have found that the Mo_6S_8 and Mo_6Se_8 clusters in $\text{Li}_{3,3}\text{Mo}_6\text{S}_8$ and $\text{Li}_{3,2}\text{Mo}_6\text{Se}_8$ are quite similar to those in other compounds of this type, and that the lithium atoms are disordered over the available small ion ring sites similar to the Cu atoms in $\text{Cu}_x\text{Mo}_6\text{S}_8$ but with some interesting differences.

Experimental

Detailed description of the synthesis of the compounds has been reported elsewhere (2). Samples of powders of the two phases were sealed in vanadium containers in a dry-helium atmosphere to avoid exposure to air and moisture.

Neutron diffraction measurements were performed on the high-resolution five-counter powder diffractometer at the NBS Reactor, with neutrons of wavelength $1.5416(3) \text{ \AA}$. The experimental conditions used to collect the data are presented in Table I. The powder profile refinement was performed using the Rietveld program (5) adapted to the five-detector diffractometer design and modified to allow the refinement of background intensity (6).

TABLE I

EXPERIMENTAL CONDITIONS USED TO COLLECT THE NEUTRON POWDER INTENSITY DATA FOR $\text{Li}_{3,3}\text{Mo}_6\text{S}_8$ AND $\text{Li}_{3,2}\text{Mo}_6\text{Se}_8$

	Monochromatic beam
Wavelength	1.5416(3) Å
Horizontal divergences	(a) In-pile collimator: 10' arc (b) Monochromatic-beam collimator: 20' arc (c) Diffracted beam-collimator: 10' arc
Monochromator mosaic spread	~15' arc
Sample container	Vanadium can ~10 mm in diameter
Angular ranges scanned by each detector	10–40, 25–60, 45–80, 65–100, 85–120
Angular step	0.05°

The high-resolution diffractometer when used with the experimental conditions described in Table I, gives Gaussian instrumental profiles over the 2θ angular range within a very good approximation. We employed for the refinement of the structures the modification of the Rietveld program describing non-Gaussian profiles with the Pearson type VII distribution, which allows the lineshape to be varied continuously from Gaussian to Lorentzian by changing one additional profile parameter (7), and found the peak profiles from $\text{Li}_{3,3}\text{Mo}_6\text{S}_8$ and $\text{Li}_{3,2}\text{Mo}_6\text{Se}_8$ were described well by the standard Gaussian function. The neutron-scattering amplitudes employed were $b(\text{Li}) = -0.214$, $b(\text{Mo}) = 0.69$, $b(\text{S}) = 0.28$, and $b(\text{Se}) = 0.80 \times 10^{-12} \text{ cm}$. Initial lattice parameters were obtained by estimate from the positions of lines at high 2θ values. Approximate values of the background parameters were obtained at positions in the patterns free from diffraction effects. The background was assumed to be a straight line with finite slope and was refined separately for each counter. This description is quite adequate for the compounds studied and for the small angular interval scanned by each counter. In the final refinements, all structural and profile parameters were refined simultaneously. Refinements were terminated when in two successive cycles the factor R_w (see Table III) varied by less than one part in a thousand. In the final refinements 14 profile, 18 structural, and 2 lattice parameters were varied.

Results

Initial atomic positions in space group $R\bar{3}$ were taken as those in $\text{Cu}_{2,94}\text{Mo}_6\text{S}_8$ (9), as the Li atoms might be expected to have similar coordination geometry to the Cu atoms. The positions of the atoms in the $\text{Mo}_6\text{S}_8/\text{Se}_8$ cluster do not differ greatly from compound to compound in the class of materials and thus the Mo and S/Se positions

did not vary significantly in the course of the refinements. Initial refinements for both compounds were performed with the Li atoms omitted. Difference Fourier syntheses employing observed and calculated structure factors from the profile fit were employed to locate the lithium atoms. As expected, they were found to occupy the "small atom" interstitial sites found to be occupied in other small ternary element Chevrel phases. The small atom sites form sets of concentric inner (Li1) and outer (Li2) rings, each with 6 available positions for Li atoms. At the lithium stoichiometries for the present compounds, the rings are only partially occupied. The difference Fourier maps indicated that for both compounds the distribution of Li scattering density was uniform on the 6 sites of a particular ring, and different on inner and outer rings. This indicated that lithium atoms occupy the available sites in each ring in a statistical fashion, and that occupancy of the outer ring sites was preferred over inner ring sites in both compounds.

The initial positions for Li1 and Li2 atoms for both compounds were taken as those for Cu1 and Cu2 atoms in $\text{Cu}_{2.94}\text{Mo}_6\text{S}_8$, based on the observed positions in the difference Fourier maps. In addition the initial occupancies were seen to be similar to those in the copper compound and were taken in the same ratio as that reported for $\text{Cu}_{2.94}\text{Mo}_6\text{S}_8$. To accommodate 3.3 Li/formula unit in the sulfide, and 3.2 Li/formula unit in the selenide, 9.9 (sulfide) and 9.6 (selenide) Li must be placed in the hexagonal unit cell. The occupancies of the two rings were varied in the refinements to conform to the stoichiometry:

$18 \times (\text{occupancy Li1 sites} + \text{occupancy Li2 sites}) = 9.9$ (sulfide) and $18 \times (\text{occupancy Li1 sites} + \text{occupancy Li2 sites}) = 9.6$ (selenide), e.g., one occupancy parameter was defined in terms of the other. Both the positions and relative occupancies of the two rings of Li atoms were found to be

TABLE II
FINAL ATOM COORDINATES FOR $\text{Li}_{3.3}\text{Mo}_6\text{S}_8$ AND $\text{Li}_{3.2}\text{Mo}_6\text{Se}_8$ IN SPACE GROUP $R\bar{3}$, HEXAGONAL CELL

	$\text{Li}_{3.3}\text{Mo}_6\text{S}_8$	$\text{Li}_{3.2}\text{Mo}_6\text{Se}_8$
Mo(18f)		
X	0.0156(2)	0.0150(2)
Y	0.1642(2)	0.1583(2)
Z	0.3977(2)	0.4004(2)
B	0.47(4)	0.63(3)
Li1(18f)		
X	0.699(7)	0.686(9)
Y	0.448(5)	0.487(8)
Z	0.364(5)	0.319(6)
B	2.6(4)	3.8(4)
OCC	0.123(9)	0.07(1)
Li2(18f)		
X	0.161(2)	0.163(2)
Y	0.280(2)	0.285(2)
Z	0.861(2)	0.861(2)
B	2.6(4)	3.8(4)
OCC	0.427(9)	0.46(1)
S1(Se1)(18f)		
X	0.3066(5)	0.3081(2)
Y	0.2745(4)	0.2762(2)
Z	0.4055(5)	0.4026(2)
B	0.29(9)	0.82(2)
S2(Se2)(6c)		
X	0.0	0.0
Y	0.0	0.0
Z	0.2126(3)	0.2106(2)
B	0.29(9)	0.82(2)
A_0	9.7690(2)	10.1948(2)
C_0	10.5986(3)	10.9591(2)
R_N	5.14	5.42
R_P	6.81	6.42
R_W	9.06	8.47
R_E	7.12	6.14

$$R_N = \frac{\sum |I(\text{obs}) - I(\text{calc})|}{\sum I(\text{obs})}$$

$$R_P = \frac{\sum |y(\text{obs}) - y(\text{calc})|}{\sum y(\text{obs})}$$

$$R_W = \left\{ \frac{\sum w [y(\text{obs}) - y(\text{calc})]^2}{\sum W [y(\text{obs})]^2} \right\}^{1/2}$$

$$R_E = \left\{ \frac{N - P + C}{\sum W [y(\text{obs})]^2} \right\}^{1/2}$$

where N = number of independent observations, P = number of parameters, C = number of constraints, y = counts at angle 2θ , I = Bragg intensities, and w = weights

somewhat different, in the final model, from those for Cu in $\text{Cu}_{2.94}\text{Mo}_6\text{S}_8$, but the general characteristics of the rings, in which Li atoms partially occupy available sites in a disordered manner, are preserved. The final atomic positions and crystallographic cell parameters for both $\text{Li}_{3.3}\text{Mo}_6\text{S}_8$ and $\text{Li}_{3.2}\text{Mo}_6\text{Se}_8$ are presented in Table II. We have constrained the isotropic thermal parameters of the like atoms in each compound to be equal to each other. The agree-

ment factors (Table II) for the final models are quite good. For the sulfide: $R_{\text{intensities}} = 5.14\%$ and $R_{\text{profile}} = 6.81$ and weighted profile agreement $R_w = 9.06$, which for agreement expected from statistics = 7.12, gives a $\psi = 1.27$. For the selenide: $R_{\text{intensities}} = 5.45\%$ $R_{\text{profile}} = 6.24\%$, and weighted profile agreement $R_w = 8.47\%$, and with an agreement based on statistics of 6.14%, $\chi = 1.38$. The observed, calculated and difference neutron diffraction profiles for $\text{Li}_{3.3}$

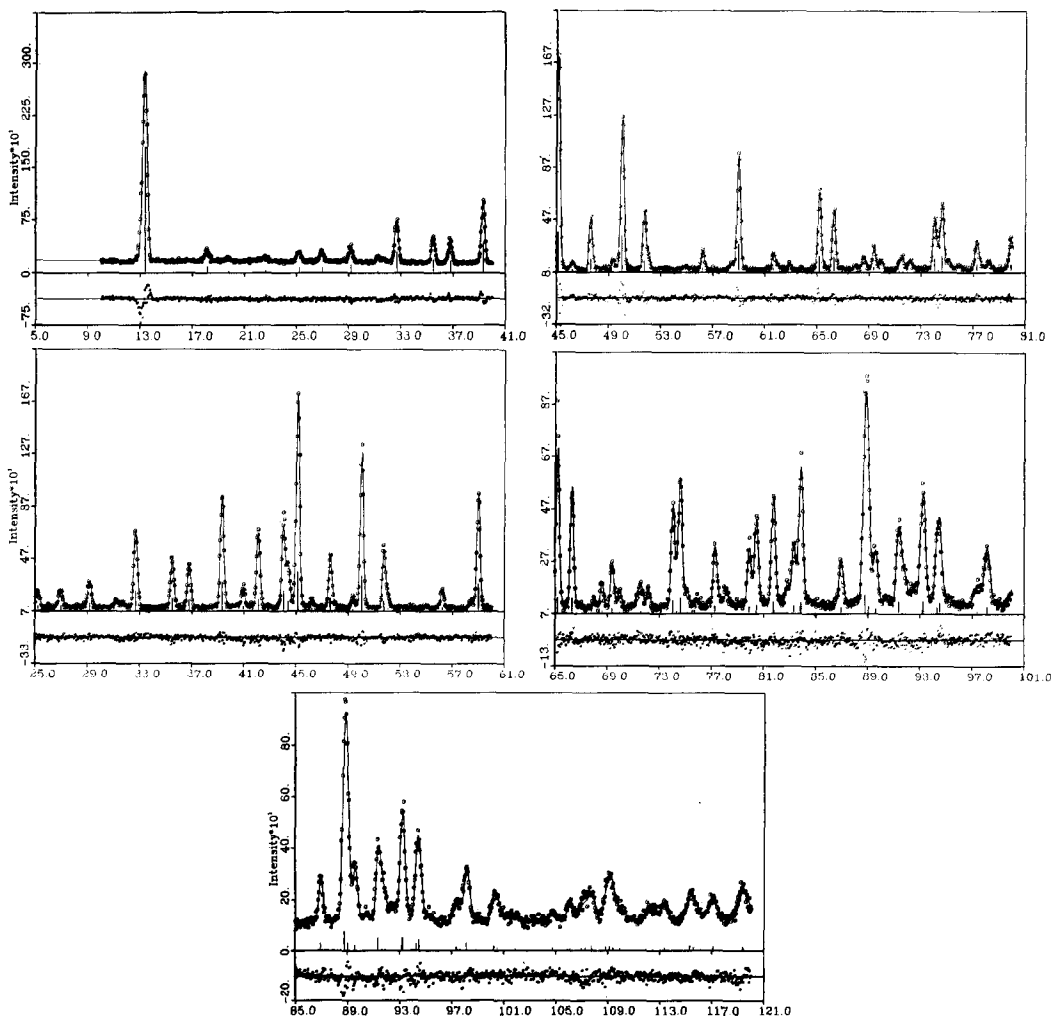


FIG. 1. Observed and calculated powder neutron diffraction profile intensities for $\text{Li}_{3.3}\text{Mo}_6\text{S}_8$. Under the profile for each of the five detectors plotted on the same scale, are the differences between the observed and calculated profiles.

Mo_6S_8 and $\text{Li}_{3,2}\text{Mo}_6\text{Se}_8$ are presented in Figs. 1 and 2, respectively. Refinements in the noncentrosymmetric space group $R\bar{3}$ did not improve the agreement factors or indicate that the atoms were not in their $R\bar{3}$ positions. A projection of the structure of $\text{Li}_{3,3}\text{Mo}_6\text{S}_8$ down the hexagonal c axis is presented in Fig. 3. In this projection the existence of three $\text{Li}_{3,3}\text{Mo}_6\text{S}_8$ chains parallel to c per unit cell is apparent. The Mo_6 octahedron and S_8 cubes are highlighted for one of the chains, and the fractional z coordinates of the atoms for another. The Li1 (inner) and Li2 (outer) rings are also apparent. For

comparison to figures published for other Chevrel phases we present in Fig. 4A the structure of one $\text{Li}_{3,3}\text{Mo}_6\text{S}_8$ unit viewed at an angle of 10° from the basal plane. The 6-atom Mo cluster is accentuated by a solid line, and the S_8 cube by a dashed line. In this projection it can be seen that the 6 Li1 positions in the inner ring are not in a plane perpendicular to c , but rather form a puckered hexagon, a feature thus far unique in the structure of small ternary atom Chevrel phases. Also visible is the outer ring (Li2), in which the atoms fall in groups of three above three below the midplane of the inner

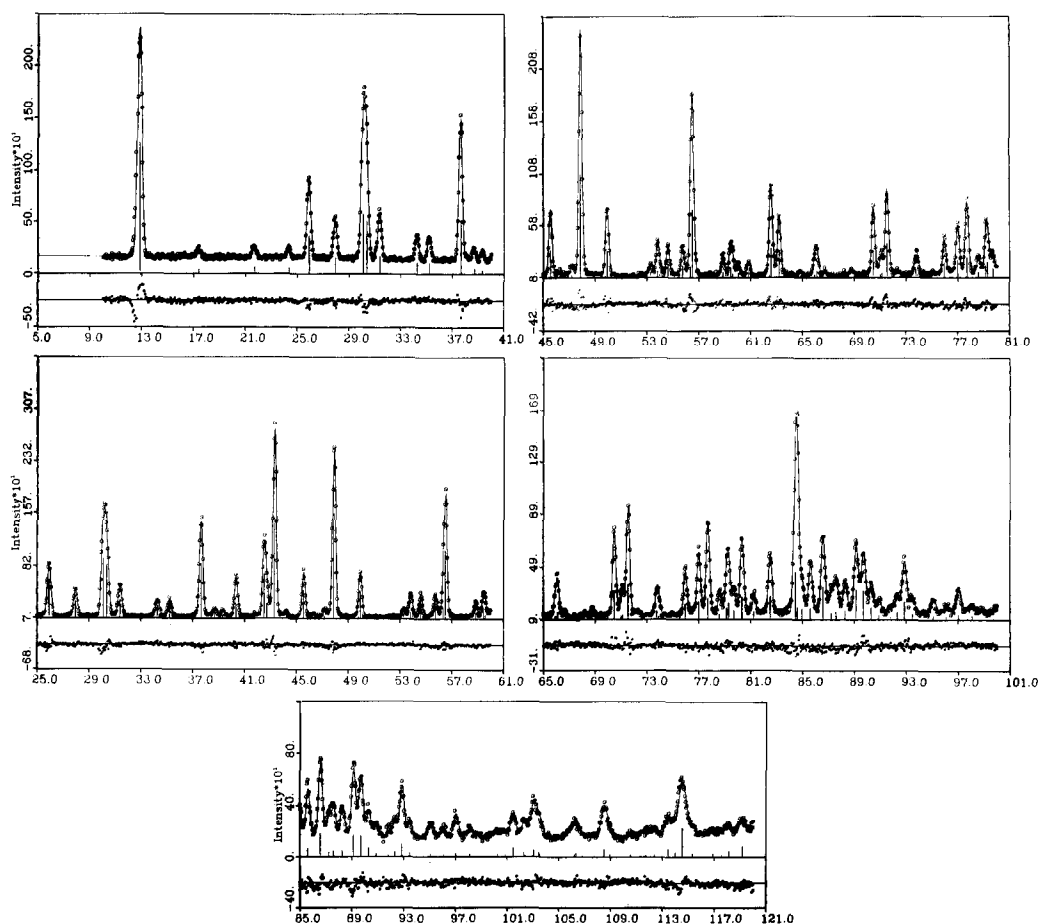


FIG. 2. Observed and calculated powder neutron diffraction profile intensities for $\text{Li}_{3,2}\text{Mo}_6\text{Se}_8$. Under the profile for each of the five detectors, plotted on the same scale, are the differences between the observed and calculated profiles.

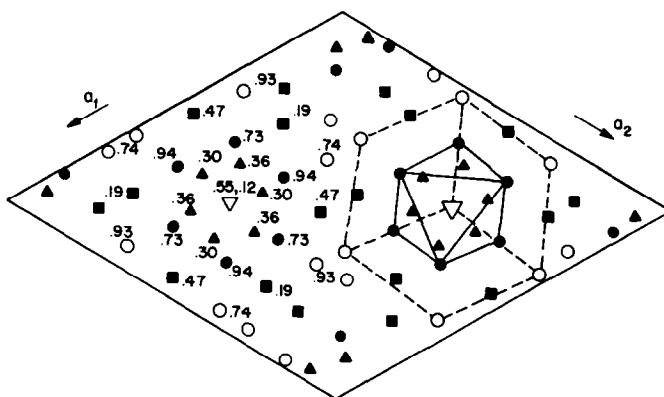


FIG. 3. Projection of the structure of $\text{Li}_{3.3}\text{Mo}_6\text{S}_8$ into the hexagonal basal plane. There are three $\text{Li}_{3.3}\text{Mo}_6\text{S}_8$ chains per unit cell running parallel to the hexagonal $(\bar{3})C$ axis. For one of the chains the S_8 cube (dashed lines) and Mo_6 octahedron (solid lines) are shown. For another of the chains, the fractional z coordinates of the atoms are shown. $\bullet = \text{Mo}$, $\blacktriangle = \text{Li1}$, $\blacksquare = \text{Li2}$, $\circ = \text{S1}$, $\nabla = \text{S2}$. Chains are displaced with respect to one another by $1/3c$ along the hexagonal axis.

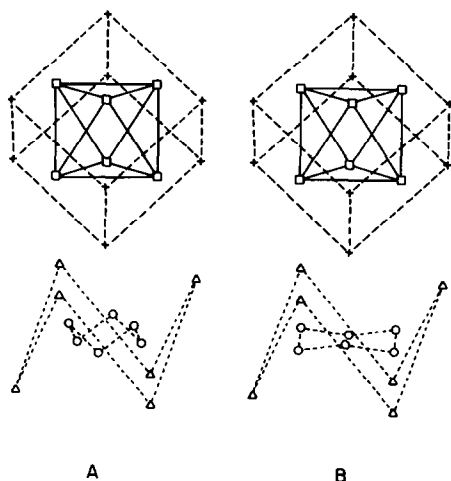


FIG. 4. $\text{Li}_{3.3}\text{Mo}_6\text{S}_8$ (A) and $\text{Li}_{3.2}\text{Mo}_6\text{Se}_8$ (B) structural units viewed at an angle of 10° from the basal plane. For both phases, Mo, Li1, and Li2 are represented by open squares (\square), circles (\circ), and triangles (\triangle). Sulfur and selenium atoms are represented by crosses ($+$). The Mo_6 octahedra and S_8 (Se_8) cubes are highlighted by solid and long dashed lines, respectively. The Li atom sites in the inner rings are connected by short dashes, as are those in the outer ring. The Li1 sites in the inner ring of the selenide are approximately coplanar, whereas those in the sulfide form a puckered hexagon.

ring. This feature is common to all small ternary atom Chevrel phases.

Further characterization of the rings can be found in Fig. 5, a detail of projections of the Li1 and Li2 positions into the hexagonal basal plane (perpendicular to c). For the sulfide (Fig. 5A), approximately 0.74(5) Li atoms are found on the average randomly distributed among the 6 sites in the inner position Li1 ring, and 2.56(5) atoms are found among the 6 sites in the outer position Li2 ring. The figure shows that the separations between sites in the inner ring are

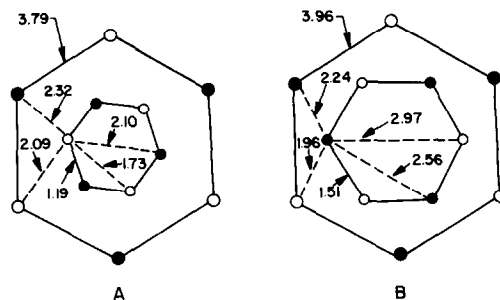


FIG. 5. The Li1 (inner) rings and Li2 (outer) rings viewed parallel to the $C(\bar{3})$ axis in (A) $\text{Li}_{3.3}\text{Mo}_6\text{S}_8$ and (B) $\text{Li}_{3.2}\text{Mo}_6\text{Se}_8$. Open circles are sites above the central plane, and closed circles sites below. Distances to near neighbors are shown. In both compounds, Li2-Li2 site distances within a ring are quite large.

quite small, even to third nearest neighbors. The Li2–Li2 site separations within the outer ring are large (3.79 Å) however the distance to the nearest Li2 site in an adjacent ring, 1.15 Å, is small. The shortest distance between sites in the inner and outer rings is 2.09 Å.

Table III presents selected interatomic distances and chalcogen–Li–chalcogen an-

TABLE III
INTERATOMIC DISTANCES IN $\text{Li}_{3.3}\text{Mo}_6\text{S}_8$ AND
 $\text{Li}_{3.2}\text{Mo}_6\text{Se}_8$

	Sulfide	Selenide
Mo–Mo	$4 \times 2.656(4)$ 3.426(3) 3.756(4)	$4 \times 2.673(6)$ 3.663(4) 3.780(5)
–S1(Se1)	2.459(4) 2.467(5) 2.487(5) 2.612(5)	2.580(3) 2.600(4) 2.603(3) 2.757(3)
–S2(Se2)	2.490(7)	2.590(4)
–Li1	3.49(5)	3.40(7)
–Li2	3.03(2) 3.14(2) 3.30(2)	3.20(2) 3.28(2) 3.49(2)
Li1–S1(Se1)	2.56(4) 2.63(7) 3.36(6)	2.1(1) 2.73(7) 3.47(8)
–S2(Se2)	2.17(5) 2.77(5)	2.61(7) 2.87(7)
–Li1	$2 \times 1.19(7)$ $2 \times 1.73(9)$ 2.1(1)	$2 \times 1.51(9)$ $2 \times 2.46(15)$ 2.97(20)
–Li2	2.09(7) 2.32(5) 2.66(7) 3.24(7) 3.28(5) 3.31(5)	1.96(7) 2.25(9) 2.84(7) 3.27(7) 3.34(9) 3.35(9)
Li2–S1(Se1)	2.36(2) 2.37(2) 2.53(2) 3.16(2) 3.63(2)	2.45(2) 2.46(2) 2.59(2) 3.24(2) 3.81(2)
–S2(Se2)	2.50(2) 3.28(2)	2.64(2) 3.38(2)
–Li2	1.15(4) $2 \times 3.79(3)$	1.13(4) $2 \times 3.96(4)$

TABLE III—Continued

	Sulfide	Selenide
S1(Se1)–S1(Se1)	$2 \times 3.485(7)$ $2 \times 3.608(6)$ $2 \times 3.637(1)$ 3.78(1)	$2 \times 3.675(3)$ $2 \times 3.725(3)$ $2 \times 3.756(1)$ 3.917(5)
–S2(Se2)	$3 \times 3.509(6)$ $3 \times 3.591(6)$ $3 \times 3.744(5)$	$3 \times 3.738(3)$ $3 \times 3.638(3)$ $3 \times 3.903(2)$
Angles in Li coordination polyhedra		
S2(Se2)–Li1–S1(Se1)	98.5(20)	104.5(28)
S2(Se2)–Li1–Si(Se1)	135.4(30)	133.4(38)
S2(Se2)–Li1–S2(Se2)	131.4(20)	114.5(30)
S1(Se1)–Li1–S1(Se1)	88.0(10)	100.0(25)
S1(Se1)–Li1–S2(Se2)	113.3(20)	118.0(30)
S1(Se1)–Li1–S2(Se2)	83.4(16)	83.6(21)
S1(Se1)–Li2–S1(Se1)	151.8(9)	153.5(10)
S1(Se1)–Li2–Si(Se1)	94.7(8)	95.2(8)
S1(Se1)–Li2–S1(Se1)	95.8(6)	96.2(6)
S1(Se1)–Li2–S2(Se2)	100.5(8)	99.8(8)
S1(Se1)–Li2–S2(Se2)	94.9(5)	94.2(5)
S1(Se1)–Li2–S2(Se2)	124.1(9)	122.1(8)

gles for the Li coordination polyhedra. The lithium coordination for both Li1 and Li2 atoms is that of a distorted tetrahedron. The Li–S bond distances range from 2.17 to 2.77 Å, and on the average are 2.49 Å. This is comparable to the Li–S separation implied in the antiferroite structure type Li_2S 2.48 Å. Representations of the Li–S coordination polyhedra are shown in Fig. 6. Mo-

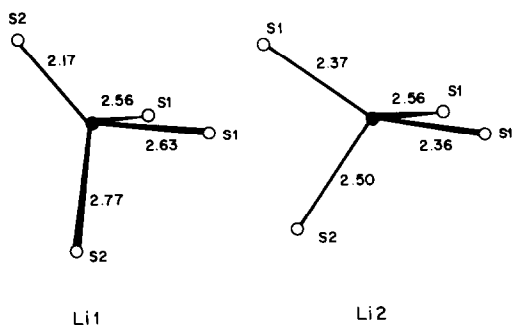


FIG. 6. Lithium–sulfur coordination for Li in inner ring (Li1) and outer ring (Li2) in $\text{Li}_{3.3}\text{Mo}_6\text{S}_8$. Closed circles, lithium; open circles, sulfur.

lybdenum atoms have 5 near neighbor sulfur atoms, at distances between 2.46 and 2.61 Å, and 4 equidistant molybdenum atoms at 2.66 Å. The distances within the Mo cluster are comparable to those found for $\text{Cu}_{2.94}\text{Mo}_6\text{S}_8$, where the Mo–Mo separations occur in sets of two which are slightly different from each other, at 2.665(2) and 2.697(2) Å. The shortest separation of Mo atoms in different clusters is 3.43 Å, and the shortest possible Li–Mo separation (to Li2), 3.03 Å.

Comparison of the entires for the sulfide and the selenide structures in Table II reveals some interesting features. In terms of fractional cell coordinates, the positions for Li2, Mo, S1, and Se1, and S2 and Se2 are virtually identical for $\text{Li}_{3.3}\text{Mo}_6\text{S}_8$ and $\text{Li}_{3.2}\text{Mo}_6\text{Se}_8$. The positions for Se1 and Se2 are determined to a greater degree of precision than those of S1 and S2 due to the relatively large scattering factor for Se. The only significant difference between the two structures concerns the distribution and positions of the Li ions. For $\text{Li}_{3.2}\text{Mo}_6\text{Se}_8$, the inner lithium ring is partially occupied with a very small number of Li atoms. On the average, 0.42(6) Li are found randomly distributed over the sites in the 6 inner ring positions, whereas 2.7(6) Li are found randomly distributed in the 6 outer ring positions. Thus, as in the sulfide, where the appropriate numbers are 0.74(5) for Li1 and 2.56(5) for Li2, the outer ring sites are strongly preferred by Li, but much more strongly so in the selenide. Due both to the small occupancy of the Li1 sites, and the large Se scattering factor, the positions of the Li1 atoms are known to relatively low precision.

For comparison, in Fig. 4B is presented the structure of one $\text{Li}_{3.2}\text{Mo}_6\text{Se}_8$ unit viewed at an angle of 10° from the basal plane. The similarity of all but the inner Li1 ring to the structure of $\text{Li}_{3.3}\text{Mo}_6\text{S}_8$ is apparent. The figure shows that the Li1 ring in the selenide is very nearly planar, as are the

inner rings in other small atom disordered phases of this type. Figure 5B shows in detail a projection of one Li1 inner and the associated Li2 outer ring into the hexagonal basal plane for $\text{Li}_{3.2}\text{Mo}_6\text{Se}_8$. It is immediately apparent that the inner ring in the selenide has a larger "diameter" (Li1—centroid on $\bar{3}$ axis distance = 1.49 Å) than that of the sulfide (Li1—centroid on $\bar{3}$ axis distance = 1.05 Å). Due to the uncertainty in the Li1 atom positions, the radius of the ring can only be specified as approximately 1.5 (*I*) Å. As in the sulfide, the Li2–Li2 position separations in $\text{Li}_{3.2}\text{Mo}_6\text{Se}_8$ are large within one ring (>3.9 Å) but small between adjacent rings (1.13 Å).

Selected interatomic distances are presented in Table III. As for the sulfide, the coordination for both Li1 and Li2 atoms is that of a distorted tetrahedron. The Li–Se bond distances range from 2.1 to 2.87 Å, with an average distance of 2.56, comparable to the Li–Se distance implied in anti-fluorite type Li_2Se , 2.61 Å. One Li1–Se1 separation at 2.10 Å is probably unrealistically short, due to uncertainty in the Li1 position, but the average Li1–Se separation 2.58 Å, is reasonable. The Li–Se coordination polyhedra are presented in Fig. 7. Molybdenum atoms have 5 near neighbor selenium atoms at distances between 2.58 and 2.60 Å and 4 equidistant molybdenum

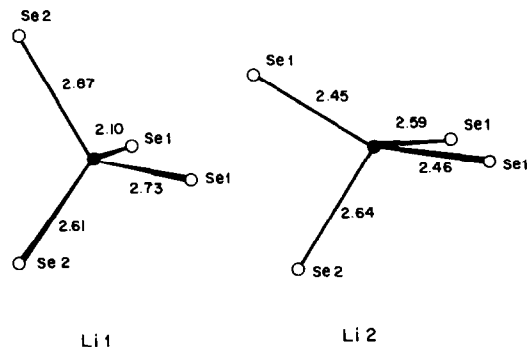


FIG. 7. Lithium-selenium coordination for Li in inner ring (Li1) and outer ring (Li2) in $\text{Li}_{3.2}\text{Mo}_6\text{Se}_8$. Closed circles, lithium; open circles, selenium.

atoms at 2.67 Å. The distances within the Mo_6 octahedral cluster are therefore essentially equivalent in $\text{Li}_{3.3}\text{Mo}_6\text{S}_8$ and $\text{Li}_{3.2}\text{Mo}_6\text{Se}_8$. The shortest separation of Mo atoms in different clusters is 3.66 Å, and the shortest possible Mo–Li position separation (to Li2), 3.20 Å.

Discussion and Conclusions

We have employed neutron diffraction powder profile analysis to determine the crystal structures of the Chevrel phases $\text{Li}_{3.3}\text{Mo}_6\text{S}_8$ and $\text{Li}_{3.2}\text{Mo}_6\text{Se}_8$. The Mo_6X_8 cluster geometries are quite similar to those found in other compounds of this type, and the lithium atoms are randomly distributed over the inner and outer ring sites as found in other small ternary element phases. The lithium atoms show a strong preference in both compounds for the outer ring (Li2) sites, although there is some occupancy of the inner ring. The $\text{Cu}_x\text{Mo}_6\text{S}_8$ compounds (9) also show a tendency toward preference of outer ring occupancy for large x , but to a much smaller degree. The geometry of the inner (Li1) ring in $\text{Li}_{3.2}\text{Mo}_6\text{Se}_8$ is similar to those found in other small ternary element phases (1) but the inner ring in $\text{Li}_{3.3}\text{Mo}_6\text{S}_8$ displays a unique puckered configuration. The structural results are contrary to the speculation (10) that the lithium ions occupy central rather than ring sites, based on apparently incorrect lattice parameter measurements.

Based on the configuration of the Li1 and Li2 rings it is possible to determine the maximum probable structurally allowed lithium stoichiometries for $\text{Li}_x\text{Mo}_6\text{S}_8$ and $\text{Li}_x\text{Mo}_6\text{Se}_8$. We begin by consideration of the Li2 rings, which have similar geometry in the two compounds, that is, very large separations within the rings but small separations between adjacent rings. Because every Li2 position has one near neighbor position at approximately 1.1 Å, only one of every pair of sites can be occupied. A

resulting Li2 concentration of 9/cell or $3/\text{Mo}_6\text{X}_8$ formula unit (F.U.) results. The observed occupation of 2.56 and 2.76 Li2/F.U. for the sulfide and selenide, respectively, indicate nearly full (85 and 92%, respectively) outer rings. For the inner rings, the geometry differs from the sulfide to the selenide, and the stoichiometry depends critically on allowed Li–Li separations in compounds of this type. The closest Li–Li separation we are aware of is in metallic Li_2ReO_3 , 2.1 Å (4); that in lithium metal is 3.0 Å, and that in Li_2S , 2.9 Å. If a 2.1-Å separation is allowable, then two Li can be squeezed into each inner Li1 ring in the sulfide, with a maximum Li1 concentration of $2/\text{Mo}_6\text{S}_8$ formula unit. This would be a very high energy configuration, however, and would require a large chemical driving force in an insertion reaction. At 0.74 Li1 per formula unit observed in $\text{Li}_{3.3}\text{Mo}_6\text{S}_8$, the inner rings are therefore relatively underoccupied (37% of available sites). For the selenide, the diameter of the inner ring is such that second nearest neighbors are relatively distant, 2.54 Å, and thus 3 of 6 of the sites per ring could be occupied. In this case, the Li1–Li2 separation is potentially the closest (1.96 Å), but that might easily be accommodated at high lithium content by a small decrease in the diameter of the inner ring or short-range order among filled and occupied Li1 and Li2 sites. The maximum Li1 concentration would then be $3/\text{Mo}_6\text{Se}_8$ formula unit, again in a high energy configuration. At 0.42 Li1 per formula unit observed for $\text{Li}_{3.2}\text{Mo}_6\text{Se}_8$, the inner ring sites are apparently greatly underoccupied (14% of the available sites). This analysis suggests maximum lithium stoichiometries of $\text{Li}_5\text{Mo}_6\text{S}_8$ and $\text{Li}_6\text{Mo}_6\text{Se}_8$ for these phases. Other factors, of course, might make compounds at those stoichiometries unstable, such as the proposal that there must be 24 or fewer electrons per Mo_6X_8 cluster (1). For $\text{Li}_x\text{Mo}_6\text{S}_8$ and $\text{Li}_x\text{Mo}_6\text{Se}_8$, a large structural change has been observed for x near 4 (2, 12) and

Schöllhorn *et al.* (3) have reported a high-lithium-content phase $\text{Li}_x\text{Mo}_6\text{S}_8$ $2.4 < x < 6$ synthesized by reaction of Mo_6S_8 with Li in liquid NH_3 . For $x > 5$ significant changes in the geometry of the Li1 inner ring in the sulfide must occur, e.g., Li1–Li1 second near neighbor separation must increase from 1.7 to greater than 2–2.1 Å.

The Mo–Mo separations in the sulfide (2.66 Å) and the selenide (2.67 Å) are of interest due both to the equality of the separations within the clusters, and their being among the shortest reported (1). Crystallographic studies of $\text{Cu}_x\text{Mo}_6\text{S}_8$ and $\text{Cu}_x\text{Mo}_6\text{Se}_8$ indicate that the Mo–Mo separations decrease in length and that two sets of initially quite different separations become more equal, as the number of copper atoms increases. This can be explained in a valence bond model (1) as being due to the gradual filling of the band of the 12 two-center Mo–Mo bonds in the cluster, which has 20 electrons in Mo_6X_8 and requires 24 electrons to be completely filled. The ternary elements donate electrons to the Mo–Mo bonds which become of more equal strength and closer to the usual Mo–Mo single-bond separation (2.59 Å) as the number of electrons per cluster approaches 24. The Mo–Mo separations in both lithium-containing compounds are consistent with a nearly filled band. Interpolation of the Mo–Mo separations to $x = 3.2$ – 3.3 for $\text{Cu}_x\text{Mo}_6\text{S}_8$, based on the results for $\text{Cu}_{2.94}\text{Mo}_6\text{S}_8$ and $\text{Cu}_{3.66}\text{Mo}_6\text{S}_8$ (9), yields 2 sets of slightly different separations of 2.66 and 2.69 Å. The fact that the Mo–Mo separations are somewhat shorter (on the average) and essentially equal in the lithium compounds is consistent with a greater ionic character for lithium than for copper, as might be expected from the greater electronegativity difference between lithium and chalcogen than copper and chalcogen.

It is of interest to consider the results of the structural studies with respect to the electrochemical Li insertion data for

$\text{Li}_x\text{Mo}_6\text{S}_8$ and $\text{Li}_x\text{Mo}_6\text{Se}_8$ (2, 12). Two solid solution phases exist near $x = 1.0$ and $x \geq 3.0$, with intermediate x values being a mixture of these phases. It has been postulated (2, 12) that the phase near $x = 1.0$ represents the preferential partial filling of the inner ring sites. Although it is tempting to comment on that postulate based on our structures in the high x phases, which find 0.74 and 0.42 Li in the inner ring sites for the sulfide and selenide, respectively, the comparisons might be incorrect. This is due to the fact that the equilibrium configuration of Li ions will be strongly dependent on Li concentration, and will be different at high x than low x . The tendency toward depopulation of the inner ring with increasing ternary atom concentration has been seen for CuMo_6S_8 (9). In $\text{Li}_x\text{Ti}_2\text{O}_4$ we have observed (11) the movement of the lithium ions from tetrahedrally coordinated to octahedrally coordinated sites as x increases from 1 to 2: the process of Li motion between tetrahedrally coordinated inner and outer rings with increasing x in the $\text{Li}_x\text{Mo}_6\text{X}_8$ phases would be a much lower energy process than in Li_xTiO_2 . With that in mind, it is likely that the lithium atoms do indeed preferentially occupy the inner rings in the low-lithium-content phases, and that that site retains most of its lithium in the high-concentration phase for the sulfide but becomes largely depopulated in the high-concentration phase for the selenide. Of course, structural studies of $\text{Li}_{1.0}\text{Mo}_6\text{S}_8$ and $\text{Li}_{1.0}\text{Mo}_6\text{Se}_8$ would be necessary to confirm this hypothesis. Of further interest for both phases would be crystal structures for phases with x greater than 3.3, especially near the expected upper Li phase limits.

References

1. K. YVON, *Curr. Top. Mater. Sci.* **3**, 53 (1979).
2. J. M. TARASCON, F. J. DiSALVO, S. W. MURPHY, G. V. HILL, E. A. RIETMAN, AND J. V. WASZAZAK, *J. Solid State Chem.* **54**, 202 (1984).

3. R. SCHÖLLHORN, M. KUMPERS, AND J. O. BESENHARD, *Mater. Res. Bull.* **12**, 781 (1977).
4. R. J. CAVA, A. SANTORO, D. W. MURPHY, S. M. ZAHURAK, AND R. S. ROTH, *J. Solid State Chem.* **42**, 251 (1982).
5. H. M. RIETVELD, *J. Appl. Crystallogr.* **2**, 65 (1969).
6. E. PRINCE, in "U. D. Tech. Note 1117" (F. J. Shorten, Ed.), pp. 8-9, National Bureau of Standards, Washington, D.C. (1980).
7. A. SANTORO, R. J. CAVA, D. W. MURPHY, AND R. S. ROTH, in "Neutron Scattering" (J. Faber, Ed.), p. 162, Conf. Proc. No. 89, American Institute of Physics (1982).
8. G. E. BACON, *Acta Crystallogr. Sect. A* **38**, 357 (1972).
9. K. YVON, A. PAOLI, R. FLUKIGER, AND R. CHEVREL, *Acta Crystallogr. Sect. B* **33**, 3066 (1977).
10. K. Y. CHEUNG AND B. C. H. STEELE, *Solid State Ionics* **1**, 337 (1980).
11. R. J. CAVA, A. SANTORO, D. W. MURPHY, S. M. ZAHURAK, AND R. S. ROTH, *J. Solid State Chem.* **53**, 64 (1984).
12. S. COLEMAN, J. R. DAHN, AND W. R. MCKINNON, private communication.
13. R. J. BEHLOCK AND W. R. ROBINSON, *Mater. Res. Bull.* **18**, 1069 (1983).